



PERGAMON

International Journal of Multiphase Flow 24 (1998) 1343–1358

---

---

International Journal of  
**Multiphase  
Flow**

---

---

## Dynamics of dual-particles settling under gravity

J. Wu\*, R. Manasseh

*CSIRO Advanced Fluid Dynamics Laboratory, Highett, Melbourne, Victoria 3190, Australia*

Received 5 November 1997; received in revised form 20 February 1998

---

### Abstract

As a first step towards understanding particle–particle interaction in fluid flows, the motion of two spherical particles settling in close proximity under gravity in Newtonian fluids was investigated experimentally for particle Reynolds numbers ranging from 0.01 to 2000. It was observed that particles repel each other for  $Re > 0.1$  and that the separation distance of settling particles is Reynolds number dependent. At lower Reynolds numbers, i.e. for  $Re < 0.1$ , particles settling under gravity do not separate.

The orientation preference of two spherical particles was found to be Reynolds number dependent. At higher Reynolds numbers, the line connecting the centres of the two particles is always horizontal, regardless of the way the two particles are launched. At lower Reynolds numbers, however, the particle centreline tends to tilt to an arbitrary angle, even if the two particles are launched in the horizontal plane. Because of the tilt, a side migration of the two particles was found to exist. A linear theory was developed to estimate the side migration velocity. It was found that the maximum side migration velocity is approximately 6% of the vertical settling velocity, in good agreement with the experimental results.

Counter-rotating spinning of the two particles was observed and measured in the range of  $Re = 0–10$ . Using the linear model, it is possible to estimate the influence of the tilt angle on the rate of rotation at low Reynolds numbers. Dual particles settle faster than a single particle at small Reynolds numbers but not at higher Reynolds numbers, because of particle separation. The variation of particle settling velocity with Reynolds number is presented. An equation which can be used to estimate the influence of tilt angle on particle settling velocity at low Reynolds number is also derived. © 1998 Published by Elsevier Science Ltd. All rights reserved.

*Keywords:* Dual-particle settling; Settling velocity; Separation distance; Particle rotation; Particle side migration; Low Reynolds number; Sedimentation

---

---

\* Corresponding author.

## 1. Introduction

Many industrial and environmental processes involve the settling of particles. A few examples are: processing mineral ores; industrial crystal precipitation; dispersion of pollutants in rivers, seas and the atmosphere; and the formation of hail in thunderstorms. Of particular interest is the behaviour of swarms of particles. Understanding the interaction of a few particles is a first step towards modelling such swarms.

Jayaweera et al. (1964) experimentally investigated small clusters of uniform spheres falling through a viscous liquid. They found that two spheres falling side by side rotate inwards and separate as they fall. When equal-sized spheres of  $Re > 1$  fall vertically, one behind the other, the rear sphere is accelerated into the wake of the leader, rotates around it and separates when the line of centres is horizontal. Thus, they tend to occupy the same horizontal plane.

In more recent years, Joseph and his colleagues (Joseph, 1994; Joseph et al., 1994) studied the motions of a few particles in Newtonian and non-Newtonian fluids using experimental observations and direct numerical simulations. They found a regime of particle-wake interactions in Newtonian fluids which they describe as drafting, kissing and tumbling. Here, the particles are sucked together by a wake (drafting), they kiss momentarily and then tumble to occupy the same horizontal plane. They noted that the mechanism of spheres tumbling into an across-the-stream arrangement is basically the same as that whereby a long body will put its broad side perpendicular to the stream in a Newtonian fluid. They also showed that the main difference between settling of particles in Newtonian and viscoelastic fluids is the existence of repulsion between nearby bodies in the Newtonian case and attraction in the viscoelastic case. This point was further emphasised in a separate paper (Feng et al., 1996).

Feng et al. (1994) used a direct numerical simulation to examine the fluid–particle interaction in two dimensions. Their simulation indicated that two circular particles interact in a number of stages while settling over a range of Reynolds numbers. Periodic solutions were found at low Reynolds numbers, while the drafting–kissing–tumbling suggested by Joseph and his colleagues was found to exist at higher Reynolds numbers. The two-dimensional periodic results are in agreement with the early observation of Jayaweera and Mason (1965) that two equal cylinders flutter as they fall for  $Re < 1$ . It is interesting to note that the flutter occurred without vortex shedding, since  $Re$  was too small. The interaction of two-dimensional cylinders (or circular particles) is much like that of spheres, in that cylinders rotate and separate as they fall, as observed both by Feng et al. (1994) and Jayaweera and Mason (1965).

The mechanism of repulsion can be understood through the dynamics of two fixed spheres placed side by side in a cross flow. Kim et al. (1993) used a three-dimensional numerical simulation to show that for a given Reynolds number in a Newtonian fluid, the two spheres are repelled when the spacing is within the order of the diameter, because of high pressure at the front stagnation point. They also showed that the two spheres are weakly attracted at intermediate separation distances, which was somewhat unknown before. They reported a torque on the fixed spheres, which is clearly related to the rotation of the freely falling spheres originally reported by Jayaweera et al. (1964).

The present study was motivated by the fact that although there is a wealth of information on the dynamics of a few particles settling under gravity, it is largely based on numerical simulations (Joseph et al., 1994; Feng et al., 1994; among others). Experimental data are still

scarce on the influence of particle proximity on settling velocity, particle separation or migration, and other practically important parameters.

In this paper, we present experimental measurements of two spherical particles settling under gravity in Newtonian fluids of various viscosities. The first objective is to quantify the motion of the spherical particles by measuring parameters of practical importance including the settling velocity, the angular velocity of particle rotation, the separation distance and the side migration velocity. These measurements are used to characterize the interaction of two settling particles and to better understand the fluid–particle process. The second objective is to use a linear theory, originally developed by Wu and Thompson (1996) for estimating lift and drag of a flat plate in creeping flows, in order to estimate the influence of the tilt angle on all the relevant particle settling parameters.

## 2. Experimental

The experiments were carried out using two square glass tanks,  $400 \times 400$  mm and  $100 \times 100$  mm in cross-section, both with a height of 600 mm. Glycerol/water solutions of various concentrations from 75% to 99% glycerol by weight were used. Four different spherical particles were used sized from 5.89 to 9.35 mm as listed in Table 1. The Delrin and Torlon particles were precision ball bearings.

Particles were launched into the fluid from a sloping plate mounted on top of each tank. Particle motion could be recorded on a Videk CCD camera with a resolution of  $1280 \times 1024$  pixels via a 486 personal computer. An infra-red beam trigger device produced a TTL signal when particles passed through the beam, triggering the recording of a digital image. Image processing software (Impro-II) was used to analyze the positions of particles from the digital images. A typical experimental set-up is outlined in Fig. 1.

Particles of the same density and diameter to be launched together were first weighed using a precision Mettler AE163 scale, to ensure that the difference in the weight was within  $\pm 0.1$  mg, or less than 0.1% of a particle weight. This was found to be important in minimising particle-settling measurement errors, especially at low Reynolds numbers.

The viscosity of glycerol water solutions is sensitive to temperature, so constant temperature monitoring in an air-conditioned room was found necessary to account for any viscosity change. Viscosity was determined by measuring the settling velocity of a known spherical particle and also checked with a Contraves Rheomat 108 rheometer. The overall uncertainty in viscosity measurement was estimated at  $\pm 5\%$ . The uncertainty in measuring particle separation and tilt angle using the digital image analysis was better than 0.1%.

Table 1  
The properties of the test spherical particles

Particle ID	A	B	C	D
Material	Delrin	Torlon	Torlon	Glass
Diameter (mm)	6.35	6.35	9.53	5.89
Density ( $\text{kg/m}^3$ )	1378	1430	1430	2603

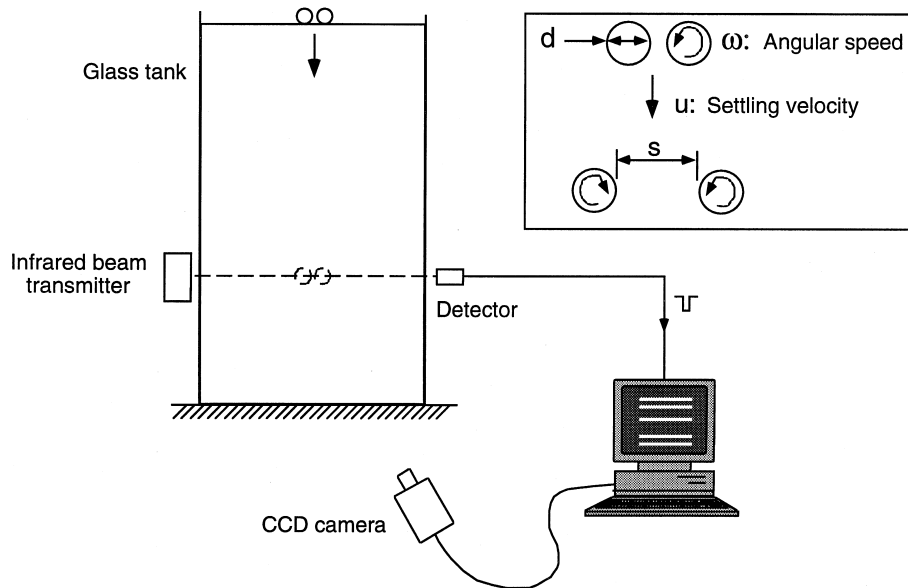


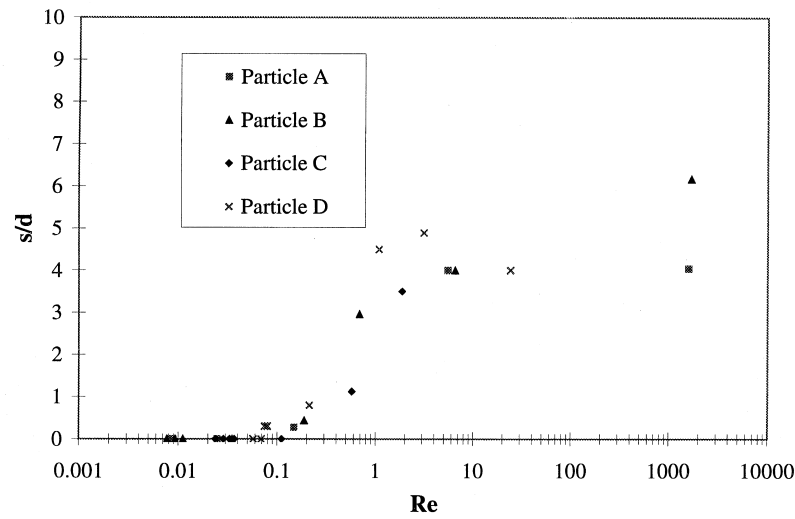
Fig. 1. Experimental set-up.

### 3. Results

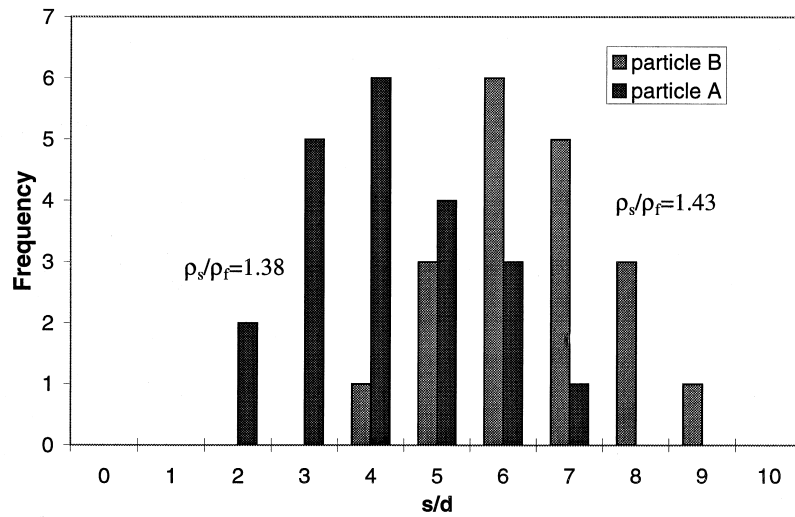
#### 3.1. Lateral separation and change in settling velocity: Reynolds number effect

When two particles are released side by side and settle in a Newtonian fluid, they may initially separate until a maximum spacing is reached; we define this spacing as the final separation distance, denoted  $s$ . For two particles launched side by side with an initial zero spacing, Fig. 2(a) shows the variation of  $s$  (normalized by particle diameter  $d$ ) with the particle Reynolds number based on the single particle settling velocity and the particle diameter. It is interesting to note that  $s$  is dependent on particle Reynolds number. At small Reynolds numbers, typically for  $Re < 0.1$ ,  $s = 0$ , implying that the repulsive force is negligible in this regime. For  $Re > 0.1$ ,  $s/d$  increases with  $Re$  until  $Re = 10$ . The variation in the data appears to be associated with the difference in particle density. A higher particle-to-fluid density ratio appears to result in a larger particle separation. This becomes more pronounced at higher Reynolds numbers, i.e.  $Re \approx 1700$ , as outlined in Fig. 2(b). The histogram was obtained from dropping particles of type A and B in water. Heavy particles tend to separate further than light particles at high Reynolds numbers.

For  $Re < 0.1$ , the repulsion is negligible since the final separation distance is zero. This is consistent with the early findings of Vasseur and Cox (1977). Using a singular perturbation technique, they analysed the interaction between two falling spherical particles at the  $Re = 0$  limit. Their results suggest that the lateral repulsion velocity approaches zero at  $Re = 0$ . The influence of the initial gap on the final separation distance was measured at  $Re = 0.02$  and plotted in the form of  $(s-s_0)/d$  vs  $s_0/d$  in Fig. 3. A negative value of  $(s-s_0)/d$  implies particles moving toward each other. The effect is rather weak, judging from the data in the graph.



(a)



(b)

Fig. 2. Separation distance of freely falling dual-particles launched side by side,  $\rho_s$  is the solid particle density and  $\rho_f$  is the fluid density: (a) variation with Reynolds number, where  $Re$  is based on the settling velocity of a single particle and particle diameter; (b) histogram of separation distance at high Reynolds number  $Re = 1700$ , particle B ( $\rho_s/\rho_f = 1.43$ ) is heavier than particle A ( $\rho_s/\rho_f = 1.38$ ).

Although it is still premature to conclude that there is some attraction at this Reynolds number, it is nevertheless quite clear that repulsion does not exist in this regime. It has been widely considered in the literature (e.g. Joseph et al., 1994) that particles always repel each other in Newtonian fluids, which is confirmed in the present study for  $Re > 0.1$ ; and that they

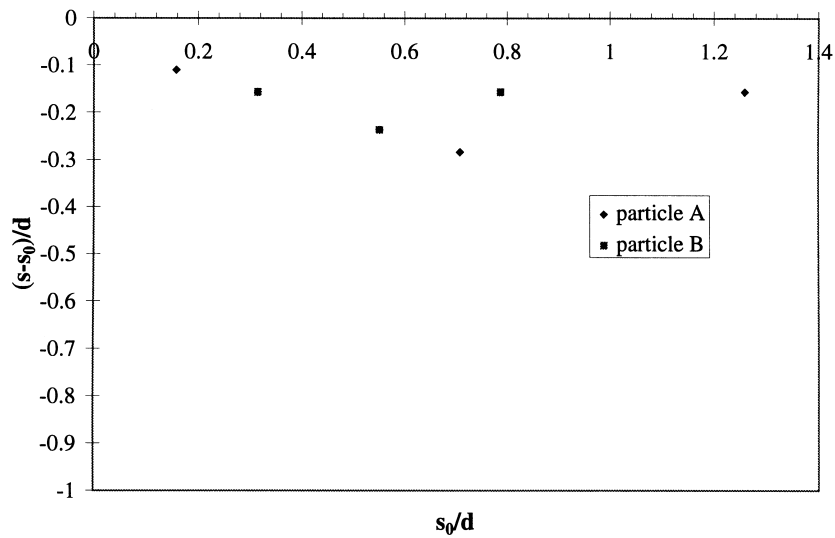


Fig. 3. Weak attraction at small Reynolds number,  $Re = 0.02$ .

attract each other in viscoelastic fluids (Feng et al., 1996, among others). The present findings extend the results of Joseph and his colleagues (Joseph, 1994; Joseph et al., 1994) and Feng et al. (1996), in showing that for a Newtonian fluid, different regimes exist for different Reynolds numbers. The present results suggest that the repulsion is a strong function of Reynolds number and that particles do not repel each other for  $Re < 0.1$ .

The ratio of the settling velocity of two particles (launched side by side with no gap between them) to that of a single particle was measured and is plotted in Fig. 4. For  $Re < 0.1$ , the

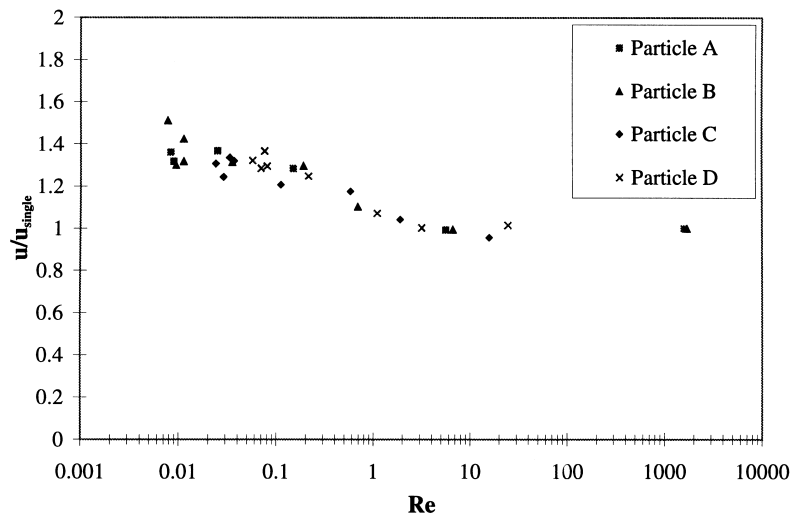


Fig. 4. Dual particle settling velocity (normalised by  $u_{single}$ ), the single particle settling velocity, vs  $Re$ . Initial gap was set to zero and all four types of particles (A, B, C and D) were used.

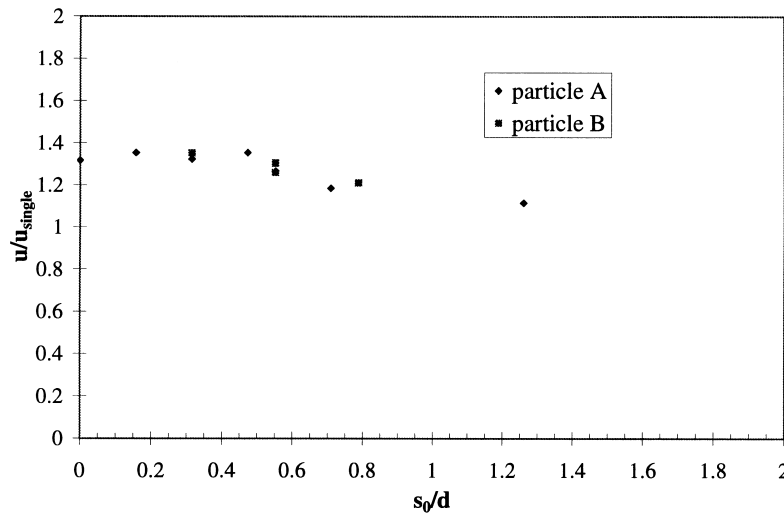


Fig. 5. Influence of the initial gap on particle settling velocity,  $Re \approx 0.02$ .

velocity of dual particles is approximately 1.3 times that of a single particle. Clearly, this is due to the fact that particles do not separate in this regime. Two particles falling together settle faster than a single particle, because of an effectively larger diameter (weight) of the two particles. It will be shown later that the settling velocity of two particles is also a function of the tilt angle of two particles; this can be estimated using a linear estimation method.

The greater settling velocity of a dual-particle configuration was also noted by Jayaweera et al. (1964). However, detailed measurements have been scarce so far. The present results help to establish the dependency of the settling velocity on Reynolds number.

For  $Re > 0.1$ , the ratio  $u/u_{\text{single}}$  decreases and approaches 1 at increasing  $Re$ . This corresponds to the fact that as  $Re$  is increased, particles separate, so the interaction between the particles becomes less significant. At low Reynolds numbers,  $u/u_{\text{single}}$  is larger than 1 for an initial spacing ( $s_0$ ) of zero. The variation of the ratio  $u/u_{\text{single}}$  with  $s_0$  for the two types of particles was measured and is shown in Fig. 5 at  $Re = 0.02$ . The influence of  $s_0$  on the settling velocity becomes less significant as  $s_0$  is increased.

### 3.2. Rotation of particles

Over a wide range of Reynolds numbers, two spherical particles settling side by side were observed to rotate, in the sense shown in Fig. 1. This rotation is obviously caused by a difference in the surface shear stresses between the side facing the other particle and the outside. The mechanism was explained with the aid of numerical simulations by Joseph et al. (1994). The rate of rotation decreases as the spheres separate at higher Reynolds numbers. To quantify the rate of rotation, particles were painted with grid lines and the angular velocity was measured by counting the number of turns a particle experienced as it fell a height of approximately 60 particle diameters. The results are plotted against Reynolds number in Fig. 6, where the angular velocity is normalised by the particle radius and the single-particle settling

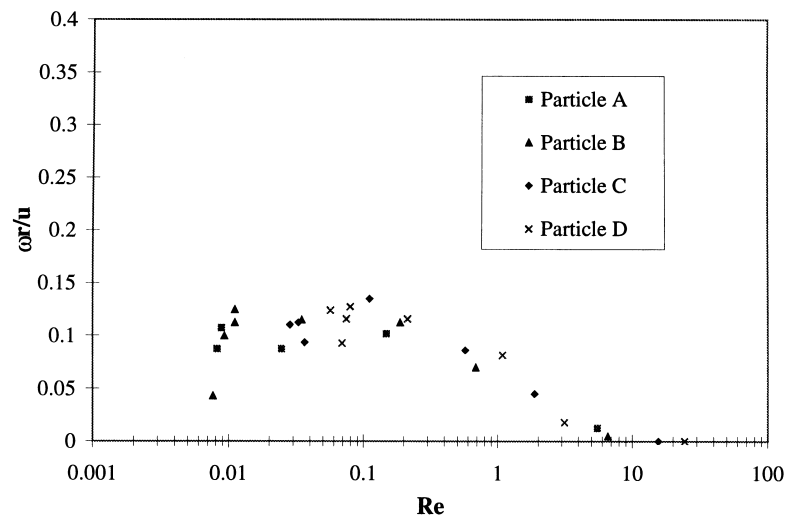


Fig. 6. Measurement of rotation of dual particles settling side by side. Non-dimensional angular velocity vs  $Re$ .  $r = d/2$ ,  $u$  is the single particle settling velocity. Initial gap was set to zero and all four types of particles (A, B, C and D) were used.

velocity. The angular velocity appears to reach the maximum of  $\omega r/u \approx 0.1-0.13$  at  $Re = 0.01-0.2$ . Increasing  $Re$  from 0.2 decreased the angular velocity. This is caused by the particle separation becoming more pronounced at  $Re > 0.2$  (Fig. 2). For  $Re < 0.008$ , the spheres showed no tendency to rotate. This scale for the rotation rate is consistent with the results of Vasseur and Cox (1977); they showed that the torque about the centre of a sphere is  $O(Re^2)$  and hence it tends to zero at  $Re = 0$ . A similar observation was reported by Jayaweera et al. (1964) at the low Reynolds number limit.

### 3.3. Orientation of particles

The orientation of the centreline connecting the centres of two falling spherical particles was found to be dependent on Reynolds number. At low Reynolds numbers, typically for  $Re < 0.01$ , the orientation of the centreline showed a high degree of uncertainty. When two particles were launched side by side, a tilt angle in the centreline usually resulted after they fell a sufficient distance. When two particles were launched with a tilt angle, the final tilt angle after the two particles travelled through the full vertical distance was usually different from the initial angle.

In order to eliminate any uncertainty caused by small differences between nominally identical spherical particles, the two particles were first dropped separately to ensure their settling velocities were indistinguishable. Thus, any change in tilt angle could not be attributed to the cumulative effect of a small difference in the settling velocity between the pair of particles. Rather, it could only be explained by the intrinsic fluid dynamical uncertainty at the low Reynolds number limit, which will be described shortly. A typical image of two particles settling in low Reynolds number flow is shown in Fig. 7. The image shows two particles (type



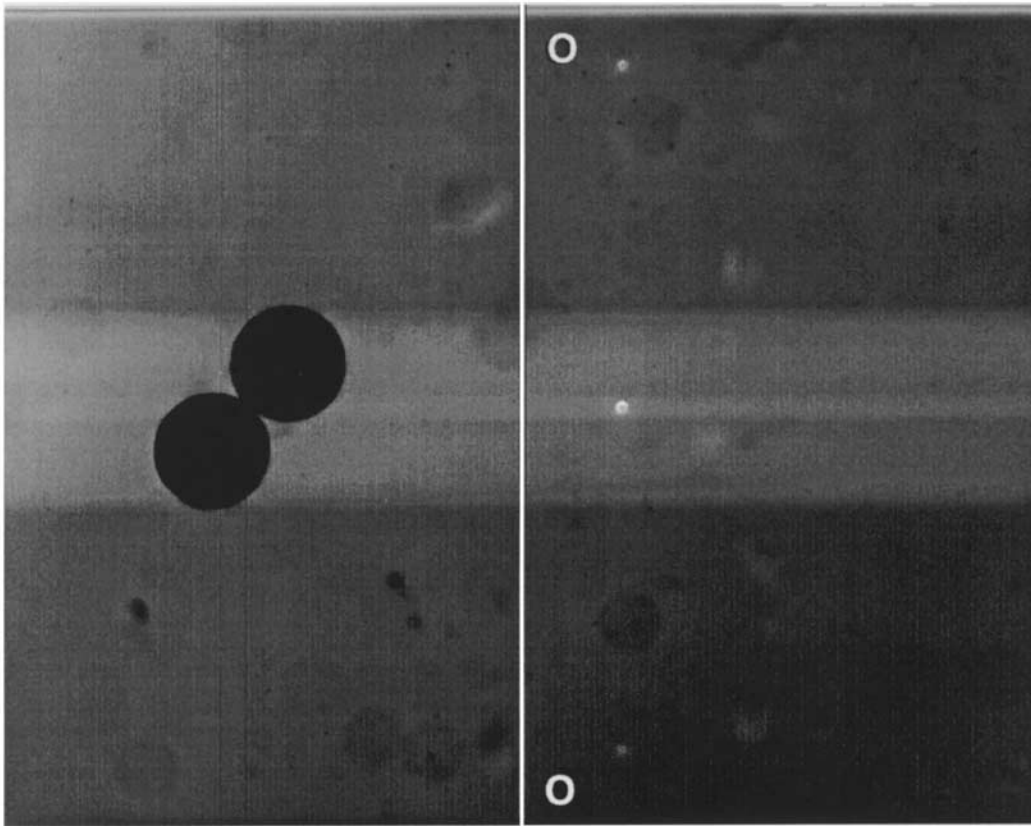


Fig. 7. Image showing two particles (type B) settling and forming a tilt angle.  $Re = 0.009$ . The centre of the frame denoted O–O is directly below the particles' drop point, thus it can be seen that they have drifted left.

B) settling and forming a tilt angle. The centre of the frame, denoted O–O, is directly below the particles' drop point; thus it can be seen that the particles have drifted leftwards. The relationship between the tilt angle and the side migration will be discussed later.

Figure 8(a) shows the histogram of tilt angle obtained from digital images recorded at  $Re = 0.009$  (using particles B, Table 1). It can be seen that the tilt angle is rather arbitrary; it is scattered across the entire range from 0 to 180°.

As Reynolds number was increased, the randomness in the tilt angle was reduced. As shown in Fig. 8(b) and 8(c), at higher Reynolds numbers, the tilt angle tended to a distribution close to 90°, i.e. particles tended to fall in the same horizontal plane, regardless of the initial condition.

It was observed that if two particles were launched with a tilt angle, the rear particle would accelerate into the lead particle and rotate around it to arrange itself in the same horizontal plane. Afterwards, the particles separated from each other, still in the same plane, for sufficiently high Reynolds numbers (approximately for  $Re > 0.1$ ).

The tendency of particles to arrange themselves in the same horizontal plane in Newtonian fluids has been reported by Joseph et al. (1994) and Feng et al. (1996), among others. The

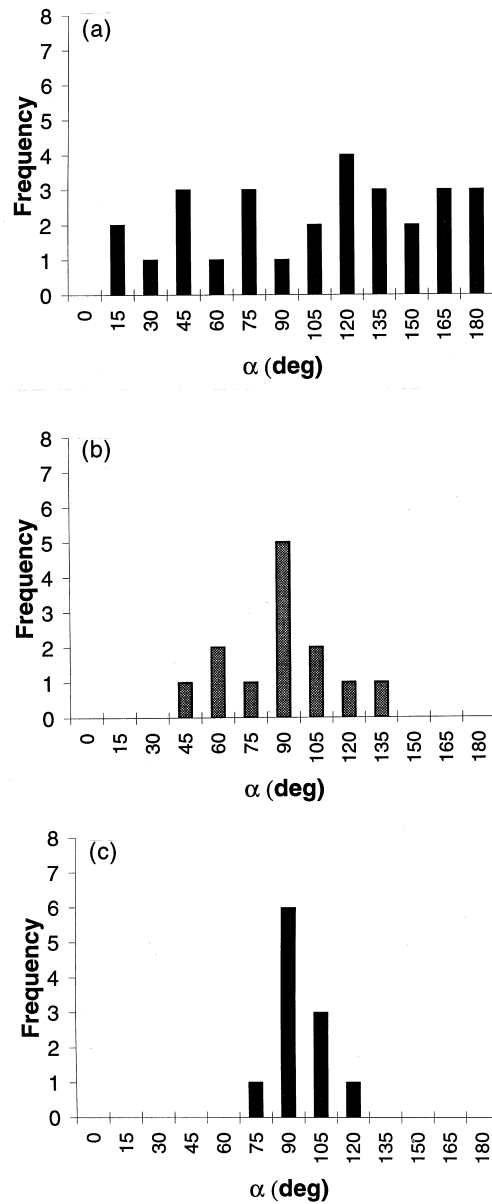


Fig. 8. Histograms of tilt angle of the centreline connecting two falling spheres: (a)  $Re = 0.009$ ; (b)  $Re = 0.07$ ; (c)  $Re = 0.25$ . Particles of type of A, B and D were used in the measurements.

mechanism is essentially similar to the case of a long body settling in a Newtonian fluid investigated by Liu and Joseph (1993). Here, a net torque is produced which tends to turn the long body to fall perpendicular to the stream. The present results, while confirming the findings of Joseph et al. (1994), Feng et al. (1996) and others, indicate that this tendency to arrange the broad side perpendicular to the stream is only visible when  $Re > 0.1$ .

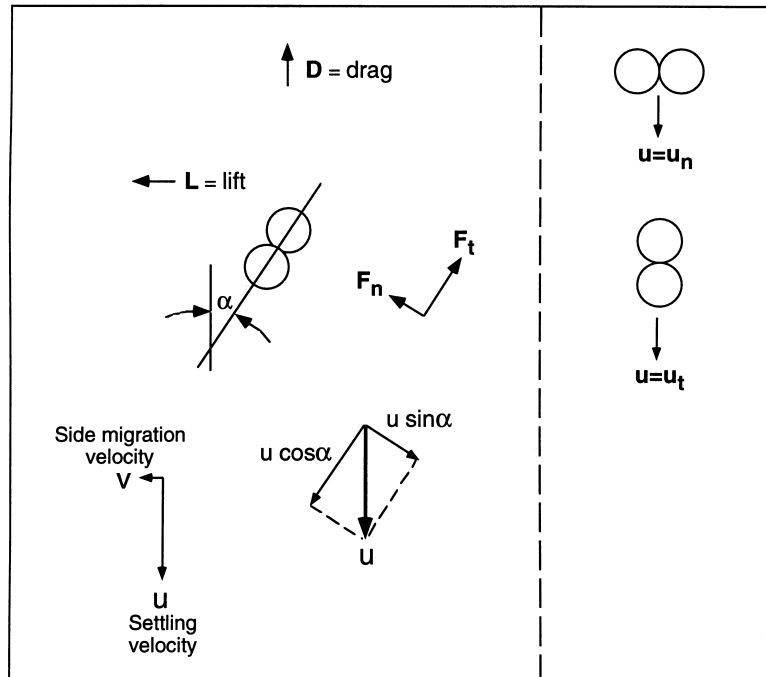


Fig. 9. Side migration of particles tilted at an angle to the horizontal plane. A linear force analysis.

At the zero Reynolds number limit, Cox (1965) concluded that the orientation of a rigid particle remains fixed indefinitely at its initial value. This implies that there should be no preference in orientation at  $Re = 0$ . In other words, particles starting with an arbitrary tilt angle will end up with the same tilt angle after falling a vertical distance. In practice, at a small finite Reynolds number, the cumulative effect of the small difference in motion around two particles is enough to produce the observed randomness in orientation. Therefore, in practical cases, the orientation of two identical particles settling together is undetermined at the low Reynolds number limit.

#### 3.4. Side migration of tilt particles: a linear model

As noted above, at low Reynolds numbers (e.g. for  $Re < 0.01$ ), the line connecting particle centres tends to tilt to an arbitrary angle. This results in a side force which tends to move particles sideways in the direction schematically drawn in Fig. 9. This was also the reason the two particles were located to the left of the origin in Fig. 7, owing to the action of the side force directed leftwards. Similar to the method of Wu and Thompson (1996), a linear superposition of solutions can be used to estimate the side migration velocity, assuming the Reynolds number is small.

As shown in Fig. 9, the velocity vector is decomposed into a tangential component,  $u \cos \alpha$  and a normal component  $u \sin \alpha$ . The forces associated with the two velocity components can be found from the Stokes drag equation,

$$F_t = c'_t \mu du \cos \alpha \text{ and } F_n = c'_n \mu du \sin \alpha,$$

where  $\mu$  is viscosity,  $c'_t$  and  $c'_n$  are velocity-independent Stokes drag coefficients, and the subscripts  $t$  and  $n$  denote tangential and normal components. The drag force  $D$  balancing the total negative buoyancy of the two particles, and the lift force  $L$  causing particle side migration are given by:

$$L = F_n \cos \alpha - F_t \sin \alpha = \frac{\mu du}{2} (c'_n - c'_t) \sin 2\alpha, \quad (1)$$

$$D = F_n \sin \alpha + F_t \cos \alpha = \mu du (c'_n \sin^2 \alpha + c'_t \cos^2 \alpha). \quad (2)$$

For the steady-state sideways component of motion, the  $L$  force is balanced by a drag,  $D'$ , obtained from (2) by substituting  $90-\alpha$  for  $\alpha$  and  $u$  with  $v$ , the side migration velocity,

$$D' = \mu dv (c'_n \sin^2(90 - \alpha) + c'_t \cos^2(90 - \alpha)),$$

so that

$$L = D'. \quad (3)$$

In addition to this, it is useful to consider the two particles settling at  $\alpha = 0$  and  $90^\circ$ . In either case, the drag in the vertical direction is balanced by the total negative buoyancy of the two particles:

$$c'_t \mu du_t = c'_n \mu du_n = 2 \times \frac{1}{6} \pi d^3 (\rho_s - \rho_f) g. \quad (4)$$

This results in

$$\frac{c'_t}{c'_n} = \frac{u_n}{u_t}, \quad (5)$$

where  $u_n$  and  $u_t$  are the settling velocities corresponding to the side-by-side and tandem configurations, respectively. The expression for the ratio of the side migration velocity to vertical settling velocity can be found using (3) and (4):

$$\frac{v}{u} = \frac{0.5(1 - u_n/u_t) \sin 2\alpha}{\cos^2 \alpha + u_n/u_t \sin^2 \alpha}. \quad (6)$$

The ratio of settling velocities of the side-by-side configuration to the tandem configuration was measured at a variety of Reynolds numbers and is plotted in Fig. 10. It can be seen that  $u_n < u_t$  and that for the Reynolds number range considered  $u_n/u_t \approx 0.9$ .

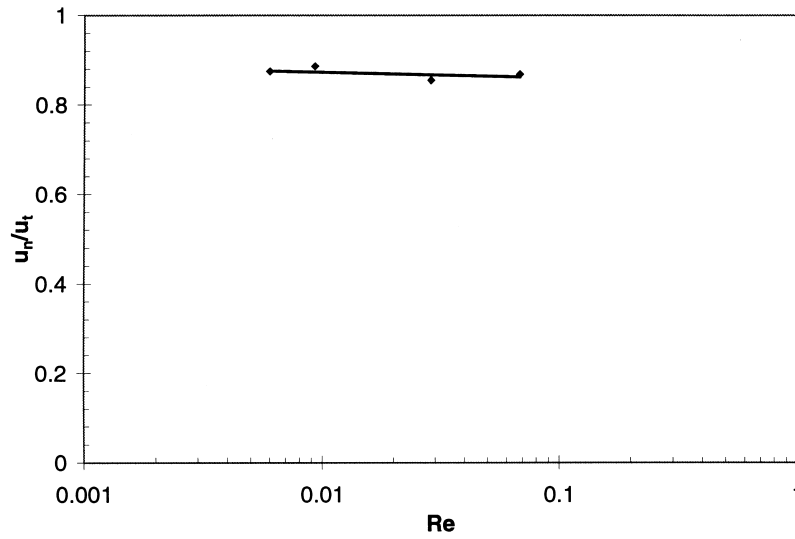


Fig. 10. Ratio of settling velocities of the side-by-side and tandem configurations. Particles A, B and D were used.

Measurements were conducted at  $Re = 0.009$  using the CCD digital image system to obtain the ratio of the side migration distance to the vertical distance the particles travelled. The tilt angle was also measured. When there was a change in the tilt angle during the fall, a mean angle was obtained by averaging the initial tilt angle and the final tilt angle. The results, tested using particle B, are plotted in Fig. 11. The prediction of (6) is also included for comparison.

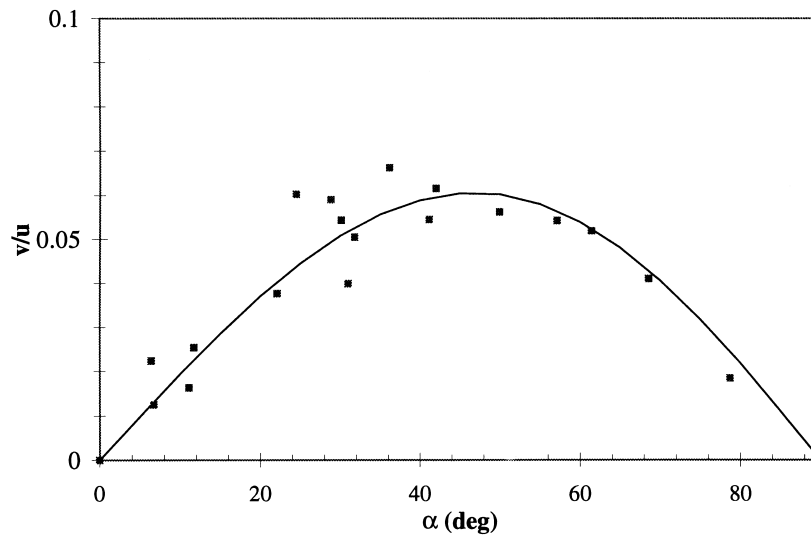


Fig. 11. Ratio of the side migration velocity to the vertical settling velocity. Points are experimental results for  $Re = 0.009$  using particle B and the curve is the prediction from the linear model, using  $u_n/u_t = 0.886$ .

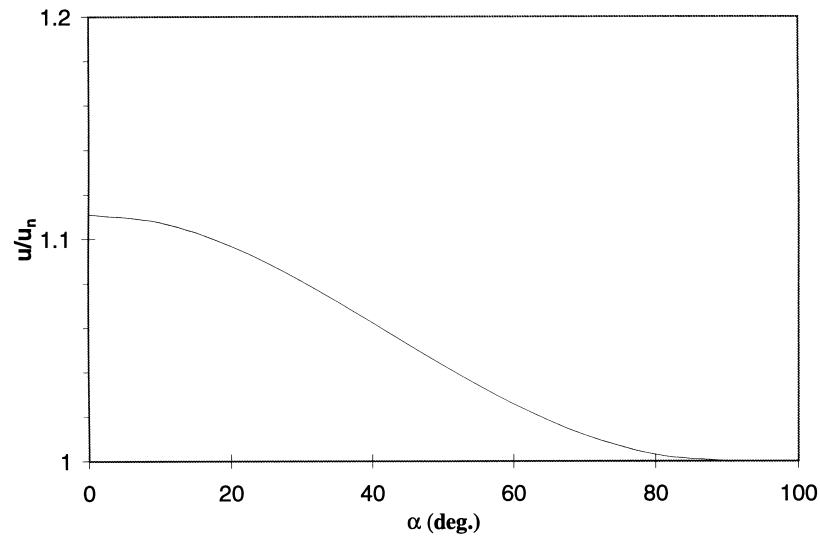


Fig. 12. Variation of settling velocity with tilt angle for  $Re < 0.1$ .

It can be concluded that the linear model agrees well with the experimental data. It is interesting to note that the maximum side migration velocity is approximately 6% of the vertical settling velocity. The theoretical maximum side migration occurs when the tilt angle is  $47^\circ$ . It differs from  $45^\circ$  because the flow is approaching the particles at an angle smaller than  $\alpha$  due to the side movement. This introduces a  $2\text{--}3^\circ$  shift in the effective  $\alpha$  near  $45^\circ$ .

### 3.5. The influence of tilt angle on settling velocity and rotation speed

The settling velocity of two particles orientated with a tilt angle can be calculated once  $u_n$  and  $u_t$  are given; using (2) and (4) one obtains:

$$\frac{u}{u_n} = \frac{1}{\sin^2 \alpha + u_n/u_t \cos^2 \alpha}. \quad (7)$$

Using the data from Fig. 10, the ratio  $u/u_n$  is calculated versus  $\alpha$ , the tilt angle, and is plotted in Fig. 12.

It is also useful to give an expression for the influence of the tilt angle on the rotation speed. Using again the linear assumption, the velocity component which is directly contributing to particle rotation at a tilt angle  $\alpha$  is  $u \sin \alpha$ . This gives

$$\omega_a = \omega \sin \alpha, \quad (8)$$

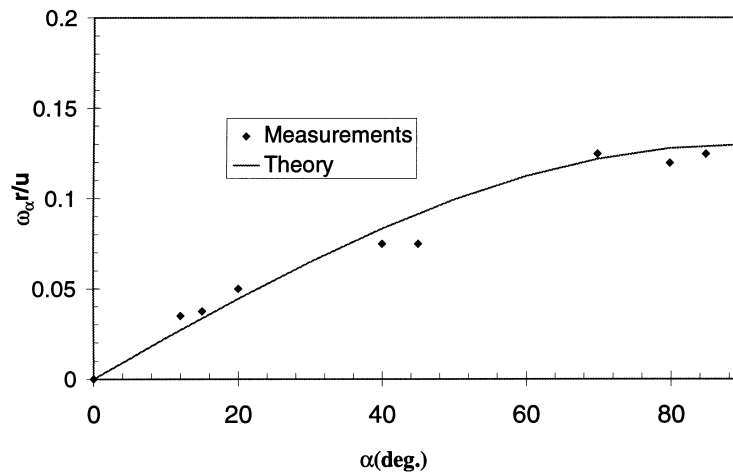


Fig. 13. Influence of tilt angle on the angular velocity, measured at  $Re = 0.035$ , particles B were used.

where  $\omega$  is the angular speed with the particles side by side and  $\omega_\alpha$  is the angular speed at a tilt angle of  $\alpha$ . Fig. 13 shows a comparison of experiments and predictions using (8); good agreement between the two is evident.

#### 4. Conclusions

The interaction between two spherical particles settling under gravity in Newtonian fluids was investigated experimentally over a Reynolds number range from 0.01 to 2000. It was observed that particles repel each other for  $Re > 0.1$ . The separation distance of particles settling under gravity was measured and found to be dependent on Reynolds number. At lower Reynolds numbers, i.e. for  $Re < 0.1$ , particles settling under gravity do not separate.

Counter-rotating spinning of two particles released side by side was also observed. The spinning was found to exist for  $Re = 0.01$ –3. The maximum angular velocity when normalised by particle settling velocity and diameter was found to be approximately 0.12–0.15 and occurs at  $Re = 0.01$ –0.1.

Dual particles settle approximately 30% faster than a single particle at small Reynolds numbers. The ratio of the dual particle settling velocity to the single particle settling velocity decreases as Reynolds number is increased. At sufficiently high Reynolds numbers, i.e.  $Re > 2$ , the ratio becomes 1. This is due to the fact that particles separate at high Reynolds numbers.

The orientation preference of the line connecting the centres of two particles was found to be Reynolds number dependent. At higher Reynolds numbers, the centreline is always horizontal, regardless of the way two particles are launched. At lower Reynolds numbers, however, the particle centreline tends to tilt to an arbitrary angle, even if the two particles are launched in a horizontal plane.

Because of the tilt, side migration of a particle pair was found to exist at low Reynolds numbers. A linear theory using the Stokes drag equation was developed to estimate the side

migration velocity and found to agree well with the experimental results. The maximum side migration velocity of two particles settling at low Reynolds numbers is approximately 6% of the vertical settling velocity and occurs when the tilt angle is approximately  $47^\circ$ . The linear theory was further used to calculate the variation of the settling velocity and the angular velocity with the tilt angle, for low Reynolds numbers.

### **Acknowledgements**

We would like to thank T. Swallow, R. Hamilton and M. Scott of CSIRO for providing the technical assistance.

### **References**

- Cox, R.G., 1965. The steady motion of a particle of arbitrary shape at small Reynolds numbers. *J. Fluid Mech.* 23, 625.
- Feng, J., Hu, H.H., Joseph, D.D., 1994. Direct simulation of initial value problem for the motion of solid bodies in a Newtonian fluid: part I—sedimentation. *J. Fluid Mech.* 261, 95–134.
- Feng, J., Huang, P.Y., Joseph, D.D., 1996. Dynamic simulation of sedimentation of solid particles in an Oldroyd-B fluid. *J. Non-Newtonian Fluid Mech.* 63, 63–88.
- Jayaweera, K.O.L.F., Mason, B.J., 1965. The behavior of freely falling cylinders and cones in a viscous fluid. *J. Fluid Mech.* 22, 709–720.
- Jayaweera, K.O.L.F., Mason, B.J., Slack, G.W., 1964. Behavior of clusters of spheres falling in a viscous fluid. *J. Fluid Mech.* 20, 121–128.
- Joseph, D.D., 1994. Interrogation of numerical simulation for modelling of flow induced microstructure. *FED-ASME* 189, 31–40.
- Joseph, D.D., Liu, Y.J., Poletto, M., Feng, J., 1994. Aggregation and dispersion of spheres falling in viscoelastic liquids. *J. Non-Newtonian Fluids Mech.* 54, 45–86.
- Kim, I., Elghobashi, S., Sirignano, W.A., 1993. Three-dimensional flow over two spheres placed side by side. *J. Fluid Mech.* 246, 465–488.
- Liu, Y.J., Joseph, D.D., 1993. Sedimentation of particles in polymer solutions. *J. Fluid Mech.* 255, 565–595.
- Vasseur, P., Cox, R.G., 1977. The lateral migration of spherical particles sedimenting in a stagnant bounded fluid. *J. Fluid Mech.* 80, 561–591.
- Wu, J., Thompson, M.C., 1996. Non-Newtonian shear-thinning flows past a flat plate. *J. Non-Newtonian Fluids Mech.* 66, 127–144.